PERGAMON

International Journal of Heat and Mass Transfer 41 (1998) 4379–4383

International Journal of HEAT and MASS TRANSFER

Technical Note
A refined solute diffusion model for columnar dendritic alloy solidification

H. Yoo[a,*], C.-J. Kim[b]

[a] *Department of Mechanical Engineering, Soong Sil University, Seoul 156-743, Korea*
[b] *Department of Mechanical Engineering, Seoul National University, Seoul 151-742, Korea*

Received 24 January 1997; in final form 10 April 1998

1. Introduction

As one of the efforts for predicting transport phenomena occurring during alloy solidification, Beckermann and coworkers [1, 2] have recently developed a sophisticated micro-macroscopic model called the multiphase model. It seems to incorporate almost all of the microscopic mechanisms present in dendritic solidification, such as back diffusion, nucleation, growth kinetics and dendrite morphology. Depending on the extent of the simplifications, various versions of the model equations have been derived and successfully applied to selected cases of interest [2–4]. Nevertheless, this model still poses an uncertainty associated with dendrite arm coarsening.

The aim of this note is to refine the solute diffusion equation in the solid phase which is a key ingredient in the micro-macroscopic model. A new solute diffusion model accounting for coarsening is proposed. It is discussed formally in comparison with the multiphase model, and validated by comparing it with well-known benchmark data as well as with an available numerical solution. In addition, the effect of coarsening on the time evolution of the local solid fraction along different cooling paths during dendritic solidification is investigated in order to show the utility of the present model.

2. Problem definition

Basic concept, detailed derivation procedure and features of the multiphase model have already been published [1, 2, 4], and thus are not repeated here. Restricting our attention to the present issue, the volume-averaged solute balance equation for a typical control (or averaging) volume shown in Fig. 1(a) was expressed as

$$\frac{\mathrm{d}}{\mathrm{d}t}(\rho_s g_s \bar{C}_s) = \rho_s C_{si}\frac{\mathrm{d}g_s}{\mathrm{d}t} + \frac{\rho_s D_s S}{l_s}(C_{si} - \bar{C}_s) \quad (1)$$

where g denotes the volume fraction; $\bar{C}$ the average concentration; D the mass diffusivity; S the interfacial area

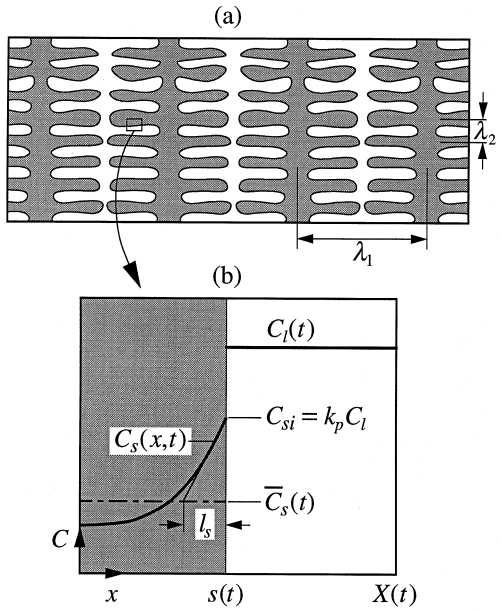

Fig. 1. Representative volume elements used for describing (a) the macroscopic, and (b) the microscopic solidification behaviors.

* Corresponding author. Tel.: +00-82-2-820-0661; Fax: +00-82-2-814-3627

PII: S0017–9310(98)00144–6

concentration; l the diffusion length. The subscripts s and l designate the solid and liquid phases, respectively. The interfacial solid concentration C_{si} is related to the liquid concentration as $C_{si} = k_p C_l$, where k_p is the equilibrium partition coefficient. In deriving equation (1), solute transport due to either diffusion or convection on the macroscopic scale has been neglected. It is observed that S is the only term capable of reflecting the effect of coarsening in equation (1). Accordingly, in the absence of back diffusion, i.e. $\rho_s D_s S/l_s = 0$, the multiphase model is unable to include the coarsening phenomenon, which motivates the present study.

Physically, the coarsening of the secondary dendrite arm spacings $\lambda_2(t)$ affects the solute redistribution process in two ways [5]. One is that it reduces the interfacial area concentration of an averaging volume, thereby making the volume-averaged diffusive flux across the interface (back diffusion) smaller. The other is that it increases the solid fraction compared with the case of a fixed arm spacing at the same heat removal condition owing to the less liquid volume to be solidified. In the multiphase model, the former is anyhow reflected through the term S, whereas the latter is not explicitly.

For later use, equation (1) is expressed in terms of the microscopic length scales. Assuming the well-mixed interdendritic and extradendritic liquids (the separate handling of them is not directly relevant to the present issue), and setting the size of a microscopic volume element as $X(t) = \lambda_2(t)/2$, a simple one-dimensional platelike secondary arm structure gives [2]

$$S = 1/X. \tag{2}$$

For such a geometry with the parabolic concentration profile in the solid [6], the diffusion length l_s is related to the interface position s as [2]

$$l_s = s/3. \tag{3}$$

It is further assumed that the solid density ρ_s is independent of time (but may depend on the concentration), which is known to be valid for dilute alloys [7]. Then equation (1) reduces to

$$\frac{d}{dt}(g_s \bar{C}_s) = C_{si}\frac{dg_s}{dt} + \frac{3D_s}{sX}(C_{si} - \bar{C}_s). \tag{4}$$

3. Modeling

It is desired that a new solute diffusion model not only incorporates the coarsening rigorously, but also is suitable for coupling with the macroscopic heat flow calculations. To this end, introduced is the postulate that the solute diffusion characteristics of the macroscopic control volume can be described, in an average sense, by those of a representative microscopic volume element (see the box in Fig. 1(a)). The volume element adopted here differs substantially from that for the microscopic conservation equation of each phase in the multiphase model [1, 2], in that the present one consists of two phases and expands with time. This type of approach is not new but has been commonly used in microsegregation modelings [6, 8]. Moreover, the solute diffusion model based on the above postulate has already been employed in the micro-macroscopic analysis [9].

Referring to the enlarged plot of the microscopic volume element in Fig. 1(b) and accepting the simplifications used for deriving equation (4), the solute conservation in the solid phase can be written as [6, 10]

$$\frac{d}{dt}(s\bar{C}_s) = C_{si}\frac{ds}{dt} + D_s\frac{\partial C_s(s,t)}{\partial x}. \tag{5}$$

Application of the parabolic concentration profile in the solid to equation (5) results in

$$\frac{d}{dt}(s\bar{C}_s) = C_{si}\frac{ds}{dt} + \frac{3D_s}{s}(C_{si} - \bar{C}_s). \tag{6}$$

Despite the differences in concept and derivation, equations (4) and (6) closely resemble each other in form. In order to verify the distinction between the multiphase and the present models, equation (6) is rewritten in terms of the solid volume fraction which is defined by $g_s = s/X$ as

$$\frac{d}{dt}(g_s\bar{C}_s) = C_{si}\frac{dg_s}{dt} + \left[\frac{3D_s}{sX} + g_s\left(\frac{1}{X}\frac{dX}{dt}\right)\right](C_{si} - \bar{C}_s). \tag{7}$$

On comparing equation (7) with equation (4), the only difference is an additional term in the square bracket which can be interpreted physically as the expansion rate of the secondary dendrite arm spacing. In actual calculations the following form may be more convenient for use instead of equation (7):

$$\frac{d\bar{C}_s}{dt} = \left[\frac{1}{g_s}\frac{dg_s}{dt} + \frac{3D_s}{g_s^2 X^2} + \left(\frac{1}{X}\frac{dX}{dt}\right)\right](C_{si} - \bar{C}_s). \tag{8}$$

Even in the absence of back diffusion ($D_s = 0$), the coarsening effect survives via the volume-expansion-rate term in equations (7) or (8), is contrary to equation (4). Note also that equation (7) degenerates to equation (4) for the fixed arm spacing (i.e. $X(t) = \text{constant}$). This implies that the solute diffusion equation of the multiphase model is a subset of the present model. Roughly speaking, the first and second terms inside the square bracket in equation (7) correspond to the two aforementioned effects of coarsening, respectively. It can be asserted at this stage that the multiphase model accounts for the coarsening effect only in part.

For evaluating the solid volume fraction g_s and the average solid concentration $\bar{C}_s$ at the prescribed temperature, the overall solute balance for the two-phase expanding volume element and the initial conditions are needed, i.e.

$$\rho_s \frac{d}{dt}(g_s \bar{C}_s) + \rho_l \frac{d}{dt}(g_s C_l) = 0 \quad (9)$$

$$g_s = 0; \quad \bar{C}_s = C_{si}, \quad C_l = C_0 \quad \text{at } t = 0. \quad (10)$$

In consequence, equations (7)–(10) constitute a set of governing equations for the present solute diffusion model in which the macroscopic solute transport is precluded. Thermodynamic relations pertinent to the phase equilibrium, density dependence on the concentration and coarsening of the secondary dendrite arms should be supplemented for the closure of modeling. The solid mass fraction corresponding to the solid volume fraction is calculated by

$$f_s = \rho_s g_s / (\rho_s g_s + \rho_l g_l). \quad (11)$$

4. Validation and application

The present model is validated by comparing the predicted eutectic volume fractions with the available data for the well-known case; directional solidification of an Al-4.9% Cu alloy. Selection of this case is not only because experimental data have been reported by Sarreal and Abbaschian [11] over a wide range of the cooling rate, but also because it is possible to discriminate the effect of coarsening with the aid of a numerical simulation [12]. Thermophysical properties, phase equilibrium diagram, density model, and coarsening model for this case have been well documented. For the consistency in comparison, all the numerical data used in the calculation were taken from those of the simulation [12].

Figure 2 shows the predicted eutectic volume fractions

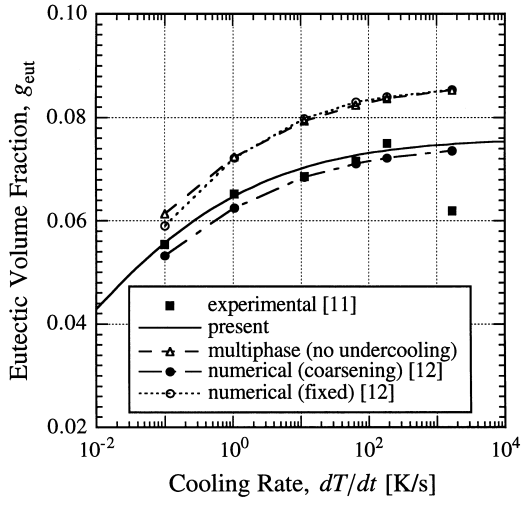

Fig. 2. Comparison of the predicted eutectic volume fractions by the present and the multiphase models with data from the experiment and numerical simulation for the directional solidification of an Al–Cu alloy.

by both the present study and the multiphase model without dendrite tip undercooling as a function of the cooling rate, together with the experimental data [11]. Two sets of the numerical results (with and without coarsening) [12] are also depicted to complement the discussion. First, all the predictions at the highest cooling rate deviate considerably from the experiment. The deviations seem to originate from the effect of undercooling in view of the work by Wang and Beckermann [4], which, however, is out of scope of the present model. It is also observed that the present model as well as the numerical simulation with coarsening agrees favorably with the experimental data over most of the cooling rates. On the other hand, predictions both from the multiphase model and from the numerical simulation without coarsening appreciably overpredict the data. The volume-expansion-rate term in equations (7) or (8), which is a unique feature of the present model, appears to be responsible for such a discrepancy. Although the present prediction nearly coincides with the numerical simulation with coarsening, the present model has an advantage of labor-saving in that a set of simplified ordinary differential equations instead of full-scale partial differential equations [12] are solved. This sort of facile character enables the present model to fit the micro-macroscopic analysis of alloy solidification, where excessive computations are faced unavoidably [3, 9], as a microscopic component.

Analytical solutions to the solute diffusion problem have been derived for a certain limiting case [5, 13], where back diffusion is absent, the equilibrium partition coefficient is constant, and the densities of the solid and liquid are equal and constant. Under the last condition, the volume and mass fractions are identical, i.e. $f_s = g_s$. One of the solutions is reproduced below [13]

$$f_s = \frac{1}{1-k_p}\left(1 - \frac{C_0}{C_l}\right) - \frac{k_p}{(1-k_p)^2}\frac{C_l^{-1/(1-k_p)}}{X(t)} \times \int_0^t X(t) C_l^{k_p/(1-k_p)} \left(1 - \frac{C_0}{C_l}\right)\frac{dC_l}{dt}\,dt. \quad (12)$$

Note that the solution reduces to the well-known Scheil equation,

$$f_s = 1 - (C_0/C_l)^{1/(1-k_p)} \quad (13)$$

only when the dendrite arm spacing is fixed. In contrast, the Scheil equation can be derived directly from the multiphase model without invoking the fixed arm spacing [4]. This is consistent with the foregoing discussion on the coarsening effect.

It is an established fact that the actual solute redistribution with finite back diffusion depends strongly on the local solidification time (or cooling rate) [10], as already shown in Fig. 2. For the limiting case of zero back

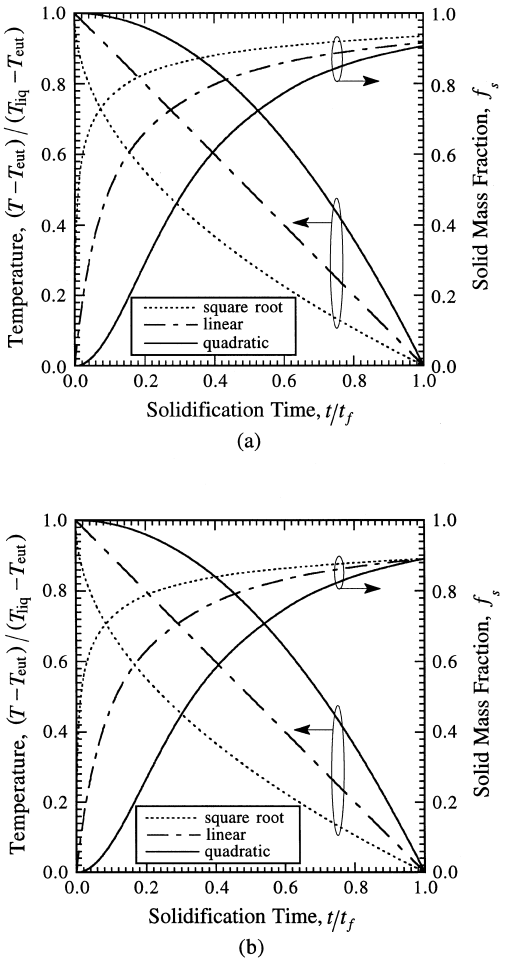

Fig. 3. Time evolutions of the solid mass fraction along different cooling paths during dendritic solidification in the absence of back diffusion: (a) with coarsening, and (b) without coarsening.

diffusion, it has long been recognized that the process is independent of time or cooling pattern, and thereupon the Scheil equation has been commonly used for evaluating the upper limit of microsegregation [10, 11]. However, this argument needs to be reassessed in view of the time-dependent nature of coarsening [5, 12, 13].

As an application of the present model, time evolution of the solid fraction f_s along different cooling paths in the absence of back diffusion is investigated. In order to focus on the effect of coarsening, calculations have been performed for a prescribed solidification time ($t_f = 100$ s for all cases under consideration) using the same numerical data with those for Fig. 2. Figure 3 depicts variations of the solid fraction during dendritic solidification (from the liquidus to the eutectic temperature) with and without coarsening, each for three cooling patterns: square root, linear and quadratic temperature-time relations. Since the overall solidification behaviors are controlled essentially by the local temperature, similar trends between Figs 3(a) and (b) appear to be reasonable. That is, the f_s curve corresponding to each cooling pattern is distinct from one another in both plots. From the physical viewpoint, it is likely that all cases yield the same f_s at the end of dendritic solidification, because all the solute rejected from the solid phase must pile up in the liquid phase eventually. In reality, f_s for each case of Fig. 3(b) coincides with one another, whereas that of Fig. 3(a) does not. This means that the dendritic growth back diffusion also depends on the cooling path because of the coarsening. Therefore, the difference in the final solid fraction (or the eutectic fraction) between Figs 3(a) and (b) can be interpreted as the net accumulated effect of coarsening.

In order to show the effect of coarsening more clearly, Fig. 3 is replotted in the liquid concentration–solid mass fraction plane (Fig. 4), which is normally termed the microsegregation curve. Interestingly, all cases without coarsening, i.e., three cooling patterns in Fig. 3(b), converge into a single curve. This can be deduced a priori from the Scheil equation since it shows a unique relation between the solid fraction and the liquid concentration. On the contrary, the microsegregation curves with coarsening differ from one another. The values of f_s with coarsening at a fixed C_l/C_0 are always larger than that without coarsening. Recall that similar differences in the eutectic fraction has been observed in Fig. 2.

Another important fact observable in Figs 3 or 4 is that rapid cooling at the early stage of solidification under a fixed solidification time, e.g. the dotted curve, is efficient

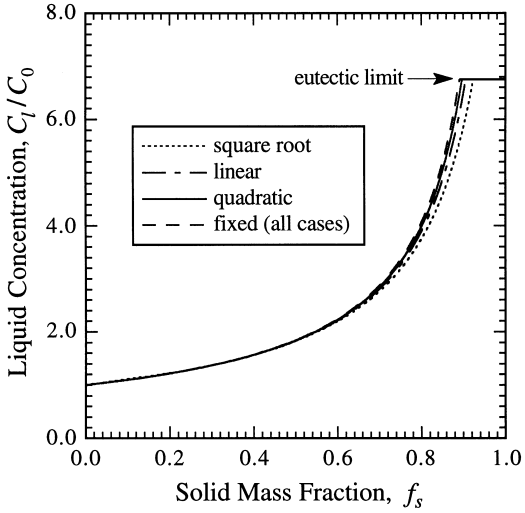

Fig. 4. Microsegregation curves corresponding to three cooling paths in Fig. 3(a) together with the case of fixed arm spacing in the absence of back diffusion.

for homogenizing the final composition of the alloy microstructures. Along such a cooling path solidification under the state of low temperature (or high interfacial concentration) lasts longer while keeping nearly the same value of the volume–expansion-rate term compared with other paths, since $X \sim t^n$ (n ranges from 0.29–0.33 approximately) in the established coarsening models [8]. This causes an increase in the average solid concentration [see equation (8)]. The higher the average solid concentration, the smaller the final eutectic fraction.

Since the evolution of latent heat predominates the heat transfer on the macroscopic scale, the coarsening which affects the local solid fraction-temperature (or concentration) relation should be carefully taken into account in the micro-macroscopic analysis of dendritic alloy solidification. In view of the compactness and consistency retained in the formulation, the present solute diffusion model is expected to be useful for such a purpose. The coupled micro-macroscopic analysis for a conduction-dominated directional casting using the present model as a microscopic component is under way.

References

[1] J. Ni, C. Beckermann, A volume-averaged two-phase model for transport phenomena during solidification, Metallurgical Transactions B 22B (1991) 349–361.

[2] C.Y. Wang, C. Beckermann, A multiphase solute diffusion model for dendritic alloy solidification, Metallurgical Transactions A 24A (1993) 2787–2802.

[3] M.C. Schneider, C. Beckermann, A numerical study of the combined effects of microsegregation, mushy zone permeability and flow, caused by volume contraction and thermosolutal convection, on macrosegregation and eutectic formation in binary alloy solidification, International Journal of Heat and Mass Transfer 38 (1995) 3455–3473.

[4] C.Y. Wang, C. Beckermann, A unified solute diffusion model for columnar and equiaxed dendritic alloy solidification, Materials Science and Engineering A171 (1993) 199–211.

[5] A. Mortensen, On the influence of coarsening on microsegregation, Metallurgical Transactions A 20A (1989) 247–253.

[6] I. Ohnaka, Mathematical analysis of solute redistribution during solidification with diffusion in solid phase, Transactions of ISIJ 26 (1986) 1045–1051.

[7] D.R. Poirier, P.J. Nandapurkar, S. Ganesan, The energy and solute conservation equations for dendritic solidification, Metallurgical Transactions B 22B (1991) 889–900.

[8] T.P. Battle, R.D. Pehlke, Mathematical modeling of microsegregation in binary metallic alloys, Metallurgical Transactions B 21B (1990) 357–375.

[9] V.R. Voller, Solidification, in: L.C. Wrobel, C.A. Brebbia (Eds.), Computational Methods for Free and Moving Boundary Problems in Heat and Fluid Flow, Elsevier Science, Oxford, 1993, pp. 189–206.

[10] W. Kurz, D.J. Fisher, Fundamentals of Solidification, 2nd ed., Trans Tech. Aedermannsdorf, Switzerland, 1989.

[11] J.A. Sarreal, G.J. Abbaschian, The effect of solidification rate on microsegregation, Metallurgical Transactions A 17A (1985) 2063–2073.

[12] S. Sundarraj, V.R. Voller, The binary alloy problem in an expanding domain: the microsegregation problem, International Journal of Heat and Mass Transfer 36 (1993) 713–723.

[13] H. Yoo, R. Viskanta, Solute redistribution limit in coarsening dendrite arms during binary alloy solidification, International Journal of Heat and Mass Transfer 40 (1997) 3875–3882.